



Audio Engineering Society

Convention Paper 7682

Presented at the 126th Convention
2009 May 7–10 Munich, Germany

The papers at this Convention have been selected on the basis of a submitted abstract and extended precis that have been peer reviewed by at least two qualified anonymous reviewers. This convention paper has been reproduced from the author's advance manuscript, without editing, corrections, or consideration by the Review Board. The AES takes no responsibility for the contents. Additional papers may be obtained by sending request and remittance to Audio Engineering Society, 60 East 42nd Street, New York, New York 10165-2520, USA; also see www.aes.org. All rights reserved. Reproduction of this paper, or any portion thereof, is not permitted without direct permission from the Journal of the Audio Engineering Society.

Forces in cylindrical metalized film audio capacitors.

P. J. Duncan¹, N. Williams², and P. S. Dodds³

¹ University of Salford, Greater Manchester, M5 4WT, UK.
p.j.duncan@salford.ac.uk

² ICW Ltd, Wrexham, Wales, LL12 0PJ, UK.
Nigel_Williams@icwLtd.co.uk

³ ICW Ltd, Wrexham, Wales, LL12 0PJ, UK.
Paul_dodds@icwLtd.co.uk

ABSTRACT

This paper is concerned with the analysis of forces acting in metalized polypropylene film capacitors in use in loudspeaker crossover circuits. Capacitors have been subjected to rapid discharge measurements to investigate mechanical resonance of the capacitor body and the electrical forces which drive the resonance. The force due to adjacent flat current sheets has been calculated in order that the magnitude of the electro-dynamic force due to the discharge current can be calculated and compared with the electrostatic force due to the potential difference between the capacitor plates. The electrostatic force is found to be dominant by several orders of magnitude, contrary to assumptions in previous work where the electro-dynamic force is assumed to be dominant.

The capacitor is then modeled as a series of concentric cylindrical conductors and the distribution of forces within the body of the capacitor is considered. The primary outcome of this is that the electrostatic forces act predominantly within the inner and outer turn of the capacitor body, while all of the forces acting within the body of the capacitor are balanced almost to zero. Experimental results where resonant acoustic emissions have been measured and analyzed are presented and discussed in the context of the model proposed.

1. INTRODUCTION AND BACKGROUND.

1.1. Introduction

The work presented in this paper is the result of collaboration between The University of Salford Acoustics Research Centre (ARC) and UK capacitor manufacturer Industrial Capacitors Wrexham Ltd (ICW) to investigate the use of metalized film capacitors in high quality audio applications. There is a great deal of debate within the loudspeaker industry about the effects that the capacitors used in the crossover circuits have on the quality of reproduced sound, and the aim of this investigation has been to understand the electrical and electro-acoustic processes of the loudspeaker and crossover capacitor combination in detail. The investigation has focused predominantly on metalized polypropylene film capacitor technologies which are available at ICW. Section 1.2 gives an outline of the literature and background to the work. Capacitors in audio applications are discussed in section 1.3, and forces in capacitors are discussed in section 1.4.

1.2. Background

There are a number of papers in which metalized film capacitor technology is discussed: Williams [1] gives a detailed account of the design issues, construction and loss mechanisms in metalized film capacitors and two papers covering capacitor technology by Sarjeant [2], [3] give an overview of types of commercially available capacitors, their typical uses, theoretical limits of energy density and details of construction. Rabuffi and Picci [4] give a description of the physics of self-healing in capacitors and Michalzyk and Bramouille [5] discuss the requirements of polypropylene films for use in energy storage applications and the trend towards eliminating weaknesses in the manufacturing process.

This work presented in this paper has focused on the use of metalized film capacitors in loudspeaker crossover applications and one of the main findings has been that the capacitors used in crossover applications exhibit varying degrees of mechanical resonance. Duncan and Dodds in [6] have shown that the resultant acoustic emissions from some of the capacitors under ac current conditions have been found to be significant, and detrimental to the overall reproduced sound quality. It therefore became necessary to carry out a theoretical

analysis of the forces acting in metalized film capacitors which would be available to excite any mechanical resonances in the physical body of the capacitor.

The principal experimental method to investigate mechanical resonance has involved rapid discharge tests where the capacitor under test is charged to its working voltage and discharged instantaneously through a thyristor. During the discharge, the rate of change of voltage was measured and used to calculate the peak discharge current, and acoustic emissions from the capacitor body were recorded using an instrumentation microphone. Having observed the resonance excited by the rapid discharge, the question then arose as to the nature and distribution of the exciting forces within the capacitor body, and whether the electrostatic or electro-dynamic force was dominant in driving the mechanical resonance.

1.3. Capacitors in Audio applications.

Metalized film capacitors find many applications in audio systems, the most common being in loudspeaker crossover circuits where the function of the capacitor is to pass high frequency components of the audio signal to the HF driver while rejecting the lower frequency components. Other applications include ac coupling of signals between audio circuits and cathode bias in valve power amplifiers. Loudspeaker manufacturers require that the capacitors used in their crossover circuits complement individual HF driver characteristics, and there is a general requirement for capacitors to be as 'transparent' as possible to the audio signal. There is considerable debate in the audio world as to which manufacturer's capacitors are most suitable and which will give the best overall audio delivery, and the main focus of this work has been a detailed investigation of metalized film capacitors in order to realize a superior audio capacitor. Much of the work has focused on mechanical vibration and resonance of the capacitor body, driven by the forces acting in a capacitor in situ in an audio circuit. This arose from discussions with loudspeaker manufacturers, and anecdotal evidence from within the industry suggested that mechanical vibration and resonance phenomena in crossover capacitors has a detrimental effect on the quality of the reproduced sound. This has been confirmed by the authors in a series of detailed subjective listening tests, the results of which are presented in [6]. Mechanical vibration and resonance effects are driven by electrostatic and electro-dynamic forces acting within the capacitor body when in use, and this is the

motivation for the following analysis of forces in metalized film capacitors, and the experimental measurements of the resulting acoustic emissions.

1.4. Forces in metalized film Capacitors.

There is a body of literature dealing with forces and vibrations in capacitors under rapid discharge conditions; Pirani and Rinaldi [7] have identified mechanical vibration of the capacitor body due to the electrical forces acting during rapid discharge, and measured the surface velocity and displacement of the walls using a laser vibrometer. The predominant driving force here is assumed to be electro-dynamic. Miyairi and Morimitsu [8] have presented work on rapid discharge of PET and Polypropylene capacitors using thyristor switching to attempt to capture misfire events in electronic ignition systems. Theoretical investigations have been carried out by Joubert et al [9], [10] and [11] in which the inhomogeneity of electro-magnetic fields inside capacitors is investigated and the consequent effect on the capacitor impedance as a function of frequency is measured. In [9], the homogeneity of the current path through a metalized film capacitor is explored to high frequencies. The capacitor is considered as a series of coaxial cylinders through which the current flows. A prediction is made that the interaction of the magnetic fields through the individual cylindrical elements ultimately affects the path of the current through the capacitor.

The second paper [10] is an investigation of the effect of electric field enhancement at the plate edges and its effect on current through the capacitor, modeled as a lumped parameter system and the final paper [11] builds on this work to develop three models which attempt to describe the high frequency impedance characteristics of capacitors. It should be noted that [9],[10] and [11] are concerned entirely with electrical resonances due to component capacitance and inductance, while the work presented in this paper is concerned with mechanical resonances, which are driven by the forces acting inside the capacitor.

Furthermore, much of the existing work outlined above on forces in capacitors has been carried out at frequencies which are several orders of magnitude above the audio frequency band, and at these frequencies, the electro-dynamic forces are likely to be predominant. However, it is unlikely that the mechanisms proposed above will have an influence on the reproduction of signals in the audio frequency band, and the analysis of forces presented in the following

section shows that electrostatic rather than electro-dynamic forces are predominant at audio frequencies.

2. ANALYSIS OF FORCES ACTING IN A METALLIZED FILM CAPACITOR

2.1. Introduction

In a metalized film capacitor under rapid discharge conditions, the total force acting between the plates will be the sum of the electrostatic force due to the charge on the capacitor plates, and the electro-dynamic force due to the current flowing in the capacitor body. Both of these forces are always attractive, and will depend on the magnitude of the applied voltage and the current during rapid discharge. The electrostatic forces are considered in section 2.2 and electro-dynamic forces in section 2.3. The outcomes are compared and discussed in section 2.4.

2.2. Electrostatic force

The force between two charged, planar capacitor plates is given by: -

$$F_e = \frac{\epsilon \cdot A \cdot V^2}{2 \cdot d^2} \text{ N} \dots\dots\dots 1$$

Where

- $F_e = \text{Force (N)}$
- $\epsilon = \text{Permittivity (F.m}^{-1}\text{)}$
- $A = \text{Area between plates (m}^2\text{)}$
- $V = \text{voltage between plates (V)}$
- $d = \text{separation of plates (m)}$

The stress applied to the dielectric between the two plates will be: -

$$\sigma = \frac{F_e}{A} = \frac{\epsilon \cdot V^2}{2 \cdot d^2} \text{ Pa} \dots\dots\dots 2$$

The compression of the dielectric due to this stress will be: -

$$\delta d = \frac{\sigma \cdot d}{Y} \text{ m} \dots\dots\dots 3$$

Where

- $Y = \text{Young's Modulus (Pa)}$

The situation is changed when the planar capacitor plates are wound into a tight cylinder. This is shown in Figure 1. Note that B is the winding “build-up” and is

the number of turns (N) multiplied by twice the film thickness (d).

The same electrostatic force will appear across each alternate plate but apart from the first turn and the last turn, the forces on alternate plates will be equal and oppositely directed and will cancel. Thus, only the first and last turns of dielectric will experience any compressive force, and this force will be acting inwards normal to the outside of the capacitor body.

Note that the diagram in figure 1 is drawn to scale and is a view of the capacitor end. At this scale (to show an adequate separation of the plates), the curvature of the winding core almost vanishes. At about a 1000:1 scale, the winding core would have a drawn diameter of 9 m.

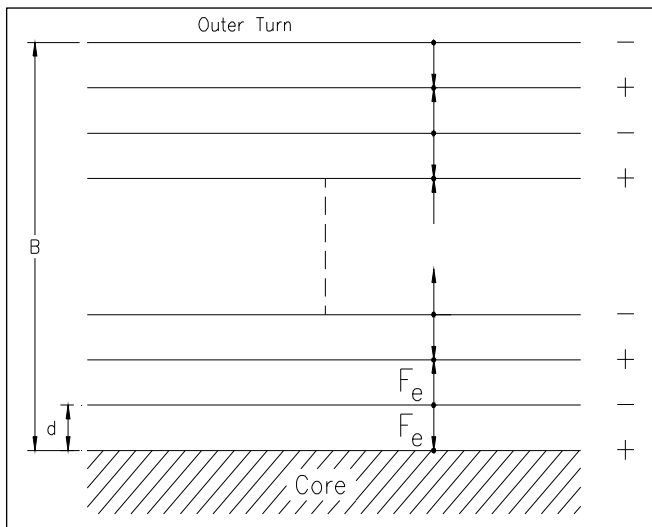


Figure 1. End view of capacitor windings.

From equation 3, it can be seen that the strain in the inner and outer turns will be the same.

The actual compressive forces on the inner turn (F_i) and the outer turn (F_o) will be: -

$$F_i = \frac{\epsilon \cdot \pi \cdot D_s \cdot W_a \cdot V^2}{2 \cdot d^2} \text{ (N)} \dots\dots\dots 4$$

And
$$F_o = \frac{\epsilon \cdot \pi \cdot D_u \cdot W_a \cdot V^2}{2 \cdot d^2} \text{ (N)} \dots\dots\dots 5$$

Where D_s = core diameter (m)
 D_u = capacitor diameter (m)
 W_a = active width of capacitor (m)

The ratio of these two forces will be given by: -

$$\frac{F_o}{F_i} = \frac{D_u}{D_s} \dots\dots\dots 6$$

The forces on either side of a particular turn will not cancel exactly because the surface area of each successive turn will increase slightly as a result of increasing circumference.

Let A_n and A_{n-1} be the surface areas of the n^{th} turn and its adjacent partner respectively. The residual force on the n^{th} turn will be: -

$$\delta F_n = \frac{\epsilon \cdot (A_n - A_{n-1}) \cdot V^2}{2 \cdot d^2} = \frac{\epsilon \cdot \pi \cdot W_a \cdot (D_n - D_{n-1}) \cdot V^2}{2 \cdot d^2}$$

Where D_n = diameter of n^{th} turn etc. (m)

But $D_n - D_{n-1} = 2 \cdot d$

Therefore
$$\delta F_n = \frac{\epsilon \cdot \pi \cdot W_a \cdot V^2}{d} \text{ (N)}$$

and the total compressive force between inner and outer turns will be: -

$$F = \delta F_n \cdot N = \frac{\epsilon \cdot \pi \cdot W_a \cdot V^2 \cdot N}{d} \text{ (N)} \dots\dots\dots 7$$

Where N = total number of turns

It can also be shown that the 3 forces are related by: -

$$F = \frac{F_o - F_i}{2} \dots\dots\dots 8$$

Equations 4, 5 and 7 represent 3 separate forces that act on the capacitor when a voltage V is applied. For illustrative purposes, the 3 forces are given below for a typical metallized polypropylene capacitor with the following parameters: -

- $d = 10^{-5} \text{ m}$
- $\epsilon_0 = 8.85 \times 10^{-12} \text{ F.m}^{-1}$
- $\epsilon_r = 2.26$
- $W_a = 34.1 \times 10^{-3} \text{ m}$
- $D_s = 9 \times 10^{-3} \text{ m}$

$$D_u = 32 \times 10^{-3} \text{ m}$$

$$N = 560$$

$$V = 260 \text{ V}$$

These parameters produce a capacitor of value approximately 4.7 μF and with the 3 electrostatic forces being: -

$$F_i = 6.52 \text{ N}$$

$$F_o = 23.18 \text{ N}$$

$$F = 8.11 \text{ N}$$

2.3. Electrodynamic force

Whenever the voltage applied to a capacitor changes, a current will flow through the capacitor. The instantaneous value of this current is given by: -

$$i = C \cdot \frac{dv}{dt} \text{ Amps}$$

This current will flow in the same direction in each electrode producing an attractive force between the electrodes. The current in each electrode will not be constant across the width of the capacitor but the sum of the currents in the two electrodes will be constant. This is illustrated in Figure 2.

The situation can be modeled if we assume two current sheets flowing in the capacitor. The situation is represented graphically in Figure 3. The capacitor is assumed planar at this point.

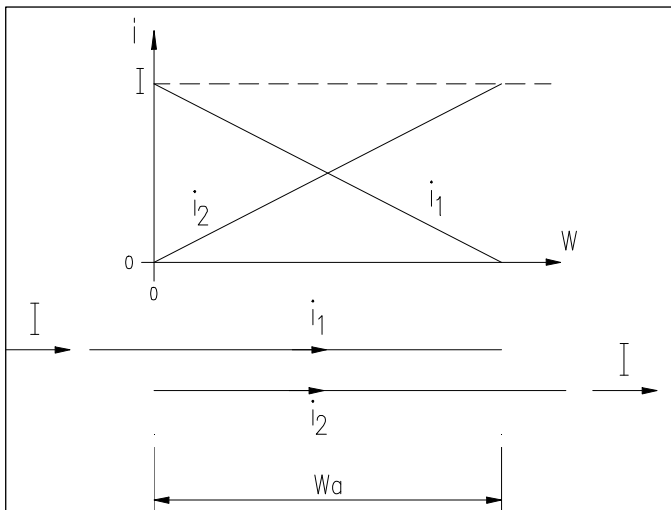


Figure 2. Schematic diagram of lateral current flow

W_a = active width of capacitor
 l_w = winding length of capacitor
 $K = K_1$ = sheet current density

$$K = \frac{i}{l_w} = \frac{C}{l_w} \cdot \frac{dv}{dt} \text{ A.m}^{-1}$$

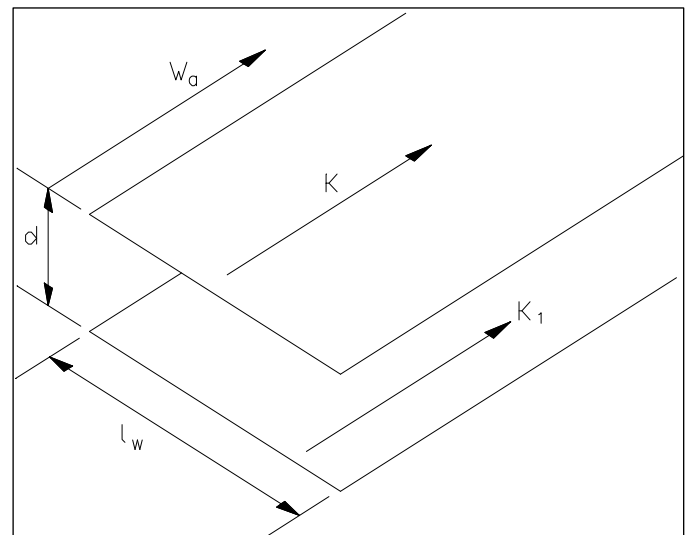


Figure 3. Schematic diagram of current flow in capacitor plates.

Note that no variation of current across the width is assumed here. If F_e is the electro-dynamic force between the plates, using the derivation given in appendix one, it can be shown that: -

$$\frac{F_d}{W_a} = \frac{\mu_0 \cdot K \cdot K_1}{2\pi} \left[2l_w \cdot \tan^{-1}\left(\frac{l_w}{d}\right) - d \cdot \ln\left(\frac{d^2 + l_w^2}{d^2}\right) \right] \text{ N.m}^{-1} \dots 9$$

$$\mu_0 = 4 \cdot \pi \cdot 10^{-7} \text{ H.m}^{-1} \text{ (permeability of free space)}$$

But, $K = K_1 = \frac{i}{l_w}$ and $l_w \gg d$

Therefore,

$$\frac{F_d}{W_a} \cong \frac{\mu_0 \cdot i^2}{\pi} \left[\frac{1}{l_w} \tan^{-1}\left(\frac{l_w}{d}\right) - \frac{d}{l_w^2} \ln\left(\frac{l_w}{d}\right) \right] \text{ N.m}^{-1}$$

and the final term in the square brackets will tend to zero therefore

$$\frac{F_d}{W_a} \cong \frac{\mu_0}{\pi} \cdot \frac{i^2}{l_w} \cdot \tan^{-1}\left(\frac{l_w}{d}\right) \quad N.m^{-1}$$

and

$$\tan^{-1}\left(\frac{l_w}{d}\right) \cong \frac{\pi}{2}$$

finally,
$$\frac{F_d}{W_a} \cong \frac{\mu_0}{2} \cdot \frac{i^2}{l_w} \quad N.m^{-1} \dots \dots \dots 10$$

The stress induced in the dielectric by this force (s) will be: -

$$\sigma = \frac{F_d}{A} = \frac{\mu_0 \cdot i^2}{2 \cdot l_w^2} = \frac{\mu_0 \cdot K^2}{2} \quad Pa. \dots \dots \dots 11$$

2.4. Comparison of electro-dynamic and electrostatic forces.

Considering a planar example of typical dimensions, we have.

- $W_a = 34 \times 10^{-3} \text{ m (34mm)}$
- $l_w = 1 \text{ m}$
- $A = 34 \times 10^{-3} \text{ m}^2$
- $d = 10^{-5} \text{ m (10}\mu\text{m)}$
- $K = 25 \text{ A.m}^{-1} \text{ or } i = 25 \text{ A}$
- $V = 250 \text{ V}$

Under these conditions, the electrostatic force F_e and the electro-dynamic force F_d are given by:

$$F_e = \frac{\epsilon \cdot A \cdot V^2}{2 \cdot d^2} = 2.1 \times 10^2 \text{ N and,}$$

$$F_d \cong 2 \cdot \pi \times 10^{-7} \times \frac{i^2}{l_w} \times W_a = 1.3 \times 10^{-5} \text{ N}$$

The ratio of the two forces is therefore

$$\frac{F_e}{F_d} = \frac{2.1 \times 10^2}{1.3 \times 10^{-5}} = 1.6 \times 10^7$$

The electrostatic force is dominant by seven orders of magnitude, and electro-dynamic forces may be safely omitted from consideration when estimating the forces acting within a metal film capacitor under rapid discharge conditions. Since the electrostatic forces acting within the body of the capacitor are always attractive and equal apart from the negligible contribution of the winding build up, the predominant force, available to initiate vibration of the capacitor body, is the electrostatic force between the outer winding and the body of the capacitor acting inwards normal to the surface of the capacitor body.

3. EXPERIMENTAL WORK.

3.1. Rapid discharge measurements

The experimental work presented here has involved measurements of acoustic emissions from capacitors under rapid discharge (impulse) excitation. Full details are given in [6] and [12]. Capacitors were charged to their working voltage then rapidly discharged via a high current thyristor. The circuit diagram for the rapid discharge experiments is shown in figure 4 below. The capacitor under test is initially charged via TH1 until charging is complete and TH1 switches off. TH2 is then pulsed to switch it on and the capacitor discharges at a rate determined by the peak current rating and the internal resistance of the circuitry which is in the order of tens of milliohms.

During and after the discharge, the resultant acoustic emissions from the capacitor body were recorded using an instrumentation microphone for analysis in the time and frequency domain.

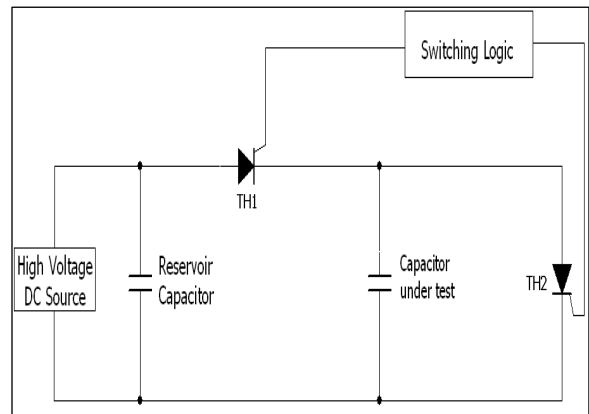


Figure 4. Circuit for rapid discharge experiments.

Typical discharge voltage and microphone output as a function of time are shown in figure 5. During the discharge, the rate of change of voltage, dV/dt gives a measure of the peak discharge current involved. In all cases, the microphone output gave an approximate decaying sinusoid signal characteristic of a damped mechanical resonance of the capacitor body. The resonance is initiated by the electrostatic force in the outer turn, which upon discharge is reduced rapidly to zero, initiating a mechanical impulse inwards towards the middle of the capacitor body.

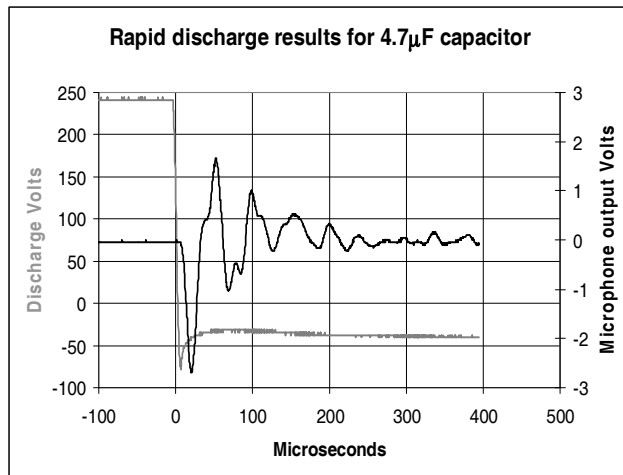


Figure 5. Time domain results for 4.7 μ F capacitor. capacitors

Time domain recordings were made for four capacitors of the same value (4.7 μ F) constructed using six micron film with four different widths.

The results were Fourier analyzed to obtain the frequency spectra of the acoustic emissions, and these are shown in figure 6. These results show a clear resonant peak for each of the capacitors in the upper audio frequency band between 14kHz and 22kHz indicative of a mechanical resonance at that frequency.

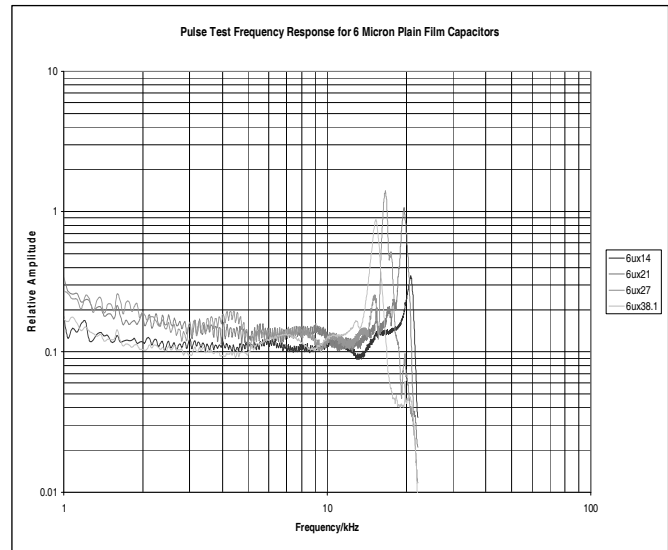


Figure 6. Frequency domain plots of acoustic emissions from four 4.7 μ F capacitors.

3.2. Reduction of discharge current using series resistance.

A further set of rapid discharge measurements were made in which a series resistor was included in the circuit to reduce the current flow during the discharge. The value of the series resistor varied from 0.1 Ω to 1 Ω . This resulted in a reduction of the peak current from 192.7 Amps with no resistor in circuit to 65 Amps with the 1 Ω resistor in circuit. The microphone output was recorded for each series resistor value and the results are shown in figure 7. It is clear from this set of results that reduction of the discharge current has not caused a reduction of the microphone output amplitude. Hence the force available to initiate the mechanical resonance does not appear to have any dependence on the discharge current. We can conclude therefore that the electrostatic force due to the Voltage rather than the electro-dynamic force due to the current is the driving force for the resonance, and is the predominant force in accordance with the theoretical analysis presented in section two.

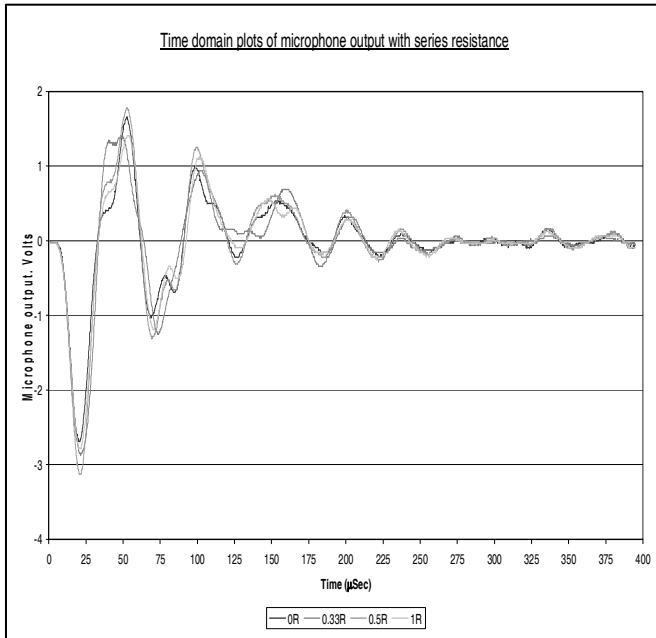


Figure 7. Time domain plots for microphone output for varying series resistance.

3.3 Vibrometer measurements.

The Salford laser vibrometer is a Polytec PSV-400 scanning vibrometer, which is a velocity measurement system described in [6]. Displacement information is derived from the recorded data using the post processing functions in the accompanying software. A series of vibrometer measurements were carried out on capacitors of varying film thicknesses and dimensions and results for the magnitude of the surface displacement as a function of frequency are given in figures 8, 9 and 10. All of the results presented show displacements in the order of tens of picometers.

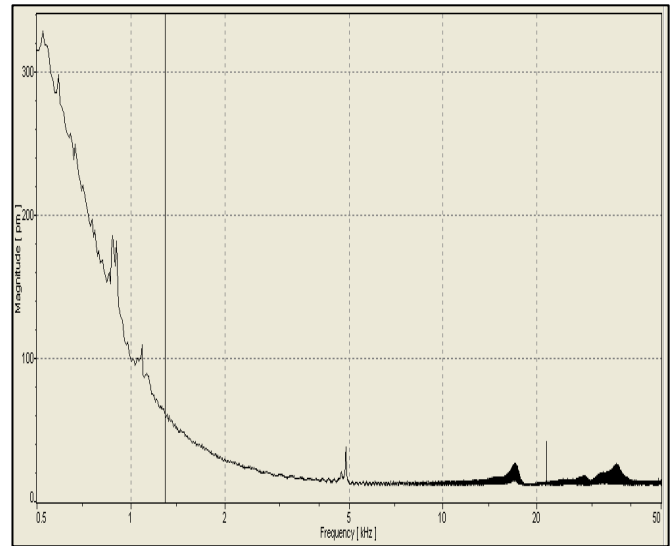


Figure 9 Magnitude displacement for 6µ dielectric.

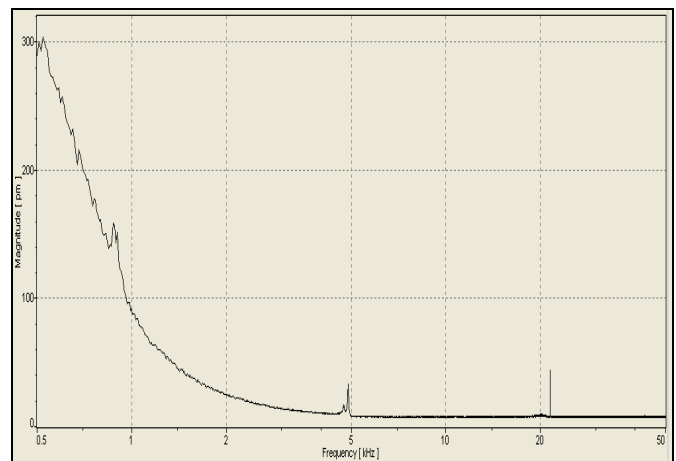


Figure 10 Magnitude displacement for 8µ dielectric.

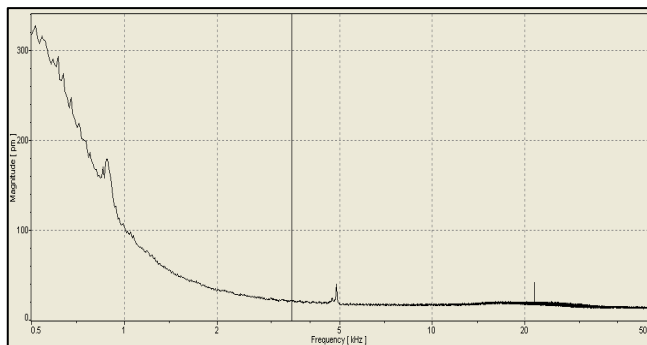


Figure 8. Magnitude displacement for 4µ dielectric.

An order of magnitude figure for the displacement due to dielectric compression by the electric force can be calculated using equation [3] and the manufacturers figure for the transverse value of Young’s modulus for the polypropylene dielectric of 4750×10^6 Pa. Calculated values for the displacement for various film thicknesses are shown in table 1.

Film thickness	displacement
4 μ m	51 μ m
6 μ m	34 μ m
8 μ m	25.5 μ m
10 μ m	21.5 μ m

Table 1

The vibrometer measurements show a displacement in the order of tens of picometers and although the correspondence between calculated and measured values are not exact, they are sufficiently close to support the mechanisms proposed.

4. SUMMARY.

An analysis of the forces in metalized film capacitors has been proposed which predicts that the dominant force acting during rapid discharge is the electrostatic force due to the Voltage rather than the electro-dynamic force due to the current as assumed in previous work in capacitor literature. In terms of the distribution of forces, the electrostatic force has the greatest influence in the outer turn of the capacitor windings since within the body of the capacitor, the forces between windings are equal and opposite and will tend to cancel to zero apart from a small contribution due to the winding build up. Experiments have been carried out where capacitors have undergone rapid discharge with the discharge voltage and acoustic emissions measured and recorded as a function of time. Analysis of the time domain data shows mechanical resonance peaks in the upper audio frequency band. Reducing the current flow during rapid discharge by inserting a series resistor in the circuit does not reduce the amplitude of the acoustic emissions indicating that the electrostatic force due to the Voltage rather than the electrodynamic force due to the current is driving the resonance in accordance with the outcomes of the analysis of the forces acting within the capacitor body presented in section two of this paper. Laser vibrometer measurements of surface displacement are in broad agreement with calculated values.

5. ACKNOWLEDGEMENTS.

The authors would like to thank Dr Olga Umnova of Salford University Acoustics Research Centre for help with solving the integrals in appendix one. The authors also wish to acknowledge the provision of test equipment and advice from B&W Speakers, KEF and Sugden Audio Ltd.

6. REFERENCES.

- 1) N. Williams, *Metallised Film Capacitors for High Frequency High Current Applications*, IEE Colloquium on Capacitors & Inductors for Power Electronics, 7th March 1996.
- 2) W.J. Sarjeant, J. Zirnheld and F.W. MacDougall, *Capacitors*, IEEE Transactions on Plasma Science (Invited Review), Vol. 26, No. 5, October 1998.
- 3) W.J. Sarjeant, *Capacitors*, IEEE Transactions on (Dielectrics &) Electrical insulation, Vol. 25 No. 5, October 1990.
- 4) M. Rabuffi and G. Picci, *Metallised polypropylene energy storage capacitors*, IEEE Transactions on Plasma Science, Vol. 30, No. 5, October 2002.
- 5) P. Michalzyk and M. Bramoulle, *Ultimate properties of polypropylene film for energy storage*, IEEE Transactions on Magnetics, Vol 39, No 1, January 2003.
- 6) P. Duncan, P. Dodds and N. Williams, *Audio capacitors. Myth or reality?* AES 124th convention Amsterdam, May 2008
- 7) S. Pirani, P. Rinaldi, *Measurements of Small Diametral Vibrations in Metallised Polypropylene Capacitors Subjected to Current Pulses, by Means of Laser Vibrometry*, IEEE Transaction on Power Delivery, Vol 18, No 1, January, 2003

- 8) K. Miyairi, N. Morimitsu, *Interpretation of Short-Circuit Discharge Current in Film Capacitors Based on an Equivalent Circuit*, IEEE Transactions on Dielectrics & Electrical Insulation, Vol 8, No 6, December 2001.
- 9) M. Joubert et al, *Magnetic field and current distribution in metallised capacitors*, American Journal of Applied Physics, Vol 76, No 9, November 1994.
- 10) M. Joubert et al, *Electric Field and Equivalent Circuit in All-Film Capacitors*, American Journal of Applied Physics, Vol 81, No 10, May, 1997.
- 11) S. Siami et al, *High frequency model for power electronics capacitors*, IEEE Transactions on Power Electronics, Vol 16, No 2, March 1997.
- 12) P. Dodds, P. Duncan, N. Williams. *Assessing the effects of loudspeaker crossover components on sound quality*, IOA Reproduced sound 22, Vol 28.Pt 8, November 2006.

7. APPENDIX 1. ELECTRODYNAMIC FORCE BETWEEN PARALLEL CURRENT SHEETS

Assume two adjacent parallel current sheets with current flowing (normal to) into the page. The current density in the upper sheet is K_1 and the current density in the lower sheet is K . Figure 1 gives a diagram of the force between two arbitrary “wires” in each current sheet represented by Kdx and K_1dx_1 .

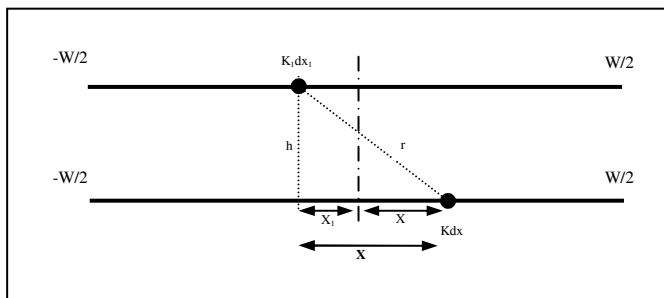


Figure 7.1. Diagram showing parallel current sheets.

The force due to the two “wires” of current Kdx and K_1dx_1 is given by

$$\frac{dF_r}{l} = \frac{dF_r}{l} \cdot \frac{h}{r} = \mu_o \frac{(Kdx)(K_1dx_1)}{2\pi r} \cdot \frac{h}{r} \dots\dots[1]$$

The distance between the “wires” r is given by $r = \sqrt{h^2 + X^2}$ so [1] becomes

$$\frac{dF_r}{l} = \mu_o \frac{KK_1h}{2\pi} \cdot \frac{dxdx_1}{h^2 + (x + x_1)^2} \dots\dots\dots[2]$$

And the force between the plates can be found by integration over x and x_1 .

$$\frac{F_r}{l} = \mu_o \frac{KK_1h}{2\pi} \cdot \int_{-\frac{w}{2}}^{\frac{w}{2}} \int_{-\frac{w}{2}}^{\frac{w}{2}} \frac{dxdx_1}{h^2 + (x + x_1)^2} \dots\dots\dots[3]$$

This is done by first changing the variables of integration so that $x=x$ and $y=x+x_1$ then [3] may be re-written as

$$\frac{F_r}{l} = \mu_o \frac{KK_1h}{2\pi} \cdot \int_{-\frac{w}{2}}^{\frac{w}{2}} \left[\int_{-\frac{w}{2}+x}^{\frac{w}{2}+x} \frac{dy}{h^2 + y^2} \right] dx \dots\dots\dots[4]$$

The ‘internal’ integral is easily solved:

$$\int_{-\frac{w}{2}+x}^{\frac{w}{2}+x} \frac{dy}{h^2 + y^2} = \left[\frac{1}{h} \text{Tan}^{-1} \left(\frac{y}{h} \right) \right]_{-\frac{w}{2}+x}^{\frac{w}{2}+x} = \frac{1}{h} \left[\text{Tan}^{-1} \left(\frac{\frac{w}{2} + x}{h} \right) - \text{Tan}^{-1} \left(\frac{-\frac{w}{2} + x}{h} \right) \right]$$

